2020

Comparative Impact of SiO2 and TiO2 Nanofillers on the Performance of Thin Film Nanocomposite Membranes

Gulsum Melike Urper-Bayram
Istanbul Technical University

Nathan Bossa
Duke University

David M. Warsinger
Purdue University, dwarsing@purdue.edu

Ismail Koyuncu
Istanbul Technical University

Mark Wiesner
Duke University

Comparative Impact of SiO_2 and TiO_2 Nanofillers on the Performance of Thin Film Nanocomposite Membranes

Gulsum Melike Urper-Bayram[1, 2, 3], Nathan Bossa[3, 4], David M. Warsinger[5], Ismail Koyuncu[1, 2,*] and Mark Wiesner[3, 4,*]

[1] Department of Environmental Engineering, Istanbul Technical University, Istanbul, TURKEY.

[2] National Research Center on Membrane Technologies, Istanbul Technical University, Istanbul, TURKEY.

[3] Department of Civil and Environmental Engineering, Duke University, Durham, NC, USA.

[4] Center for the Environmental Implications of Nano Technology (CEINT), Duke University, Durham, NC, USA.

[5] School of Mechanical Engineering, Birck Nanotechnology Center, Purdue University, Lafayette, IN, USA.

Abstract

Nanoparticle additions can substantially improve the performance of Reverse osmosis and nanofiltration Polyamide (PA) membranes. However, the relative impacts of leading additives are poorly understood. In this study we compare the effects of TiO_2 and SiO_2 nanoparticle as nanofillers in PA membranes with respect to permeate flux and the rejection of organic matter and salts. Thin film nanocomposite (TFN) PA membranes were fabricated using similarly-sized TiO_2 $(15\ \text{nm})$ and SiO_2 $(10-20\ \text{nm})$ nanoparticles (NPs), introduced at four different nanoparticle concentrations (0.01 %, 0.05 %, 0.2% and 0.5 % w/v). Compared with PA membranes fabricated without NPs, membranes fabricated with nanofillers improved membranes hydrophilicity, membrane porosity and consequently the permeability. Permeability was increased by 24% and 58% with the addition of TiO_2 and SiO_2, respectively. Rejection performance and fouling behavior of the membranes was examined with salt ($MgSO_4$ and NaCl) and organic matter (humic acid (HA) and tannic acid (TA)). The addition of TiO_2 and SiO_2 nanofillers to the PA membranes improved the permeability of these membranes and also increased the rejection of $MgSO_4$, especially for TiO_2 membranes. The addition of TiO_2 and SiO_2 to the membranes

exhibited a higher flux and lower flux decline ratio than the control membrane in organic matter solution filtration. TFN membranes' HA and TA rejections were at least 77% and 71% respectively. The surface change properties of nanoparticles appear to play a dominant role in determining their effects as nanofillers in the composite membrane matrix through a balance of changes produced in membrane pore size and membrane hydrophilicity.

Keywords : Thin Film Nanocomposite (TFN), Polyamide, TiO_2, SiO_2, Comparison, Nanofiltration.

***Corresponding author:**

Phone: 919-660-5292; fax: 919-660-5219; e-mail: wiesner@duke.edu (M. Wiesner).

Phone:212-285-3473; fax: 212-285-6667; e-mail: koyuncu@itu.edu.tr (I. Koyuncu).

Cite as:

Urper-Bayram, G.M., Bossa, N., Warsinger, D.M., Koyuncu, I. and Wiesner, M., 2020. Comparative impact of SiO2 and TiO2 nanofillers on the performance of thin-film nanocomposite membranes. *Journal of Applied Polymer Science*, *137*(44), p.49382.

Abbreviations

TFC	Thin film composite	BPO	Benzoyl Peroxide
NF	Nanofiltration	TFN	Thin Film Nanocomposite
UF	Ultrafiltration	NOM	Natural Organic Matter
RO	Reverse Osmosis	NC	Nanocomposite
PA	Polyamide	IP	Interfacial Polymerization
HA	Humic acid	FRR	Flux Recovery Ratio
TA	Tannic acid	FDR	Flux Decline Ratio
MPD	m-phenylenediamine	SEM	Scanning Electron Microscopy
IPC	isophthaloyl chloride	FTIR	Fourier Transform Infrared Spectrometer
THF	tetrahydrofuran	ZPC/PZC	Zero Point of Charge

Graphical Abstract

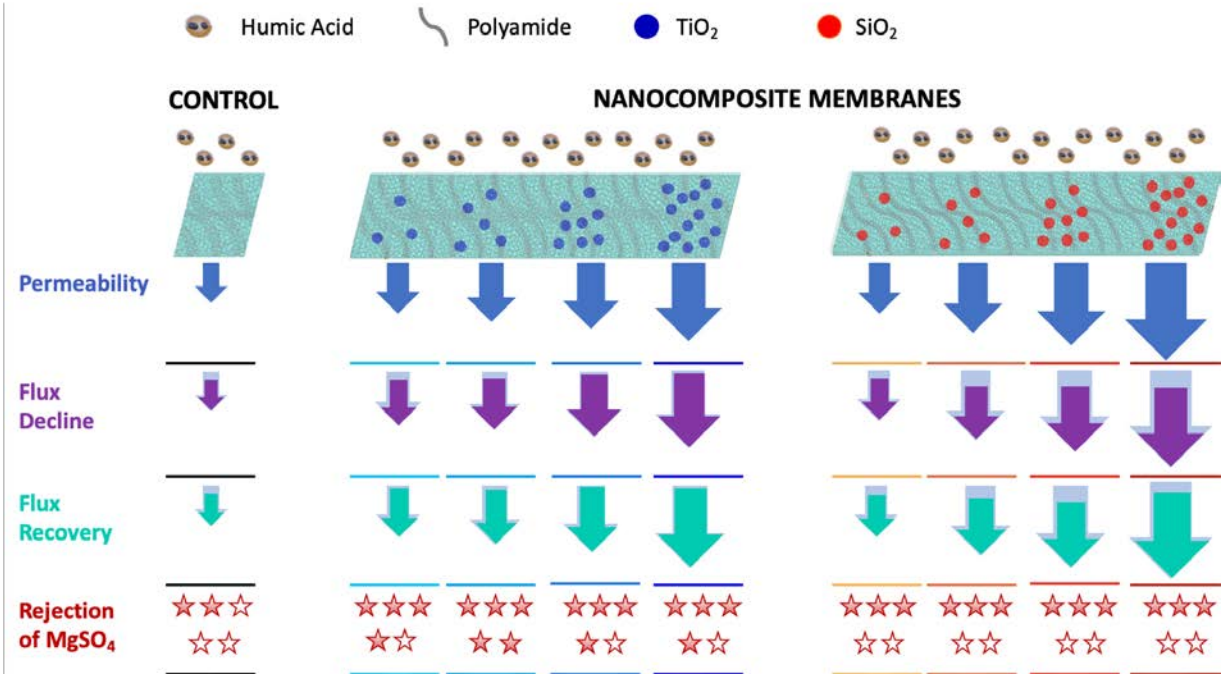

1. Introduction

Membrane technologies are broadly used for drinking water treatment, wastewater treatment, reclamation and reuse. Polyamide (PA) is the dominant polymer of choice for nanofiltration (NF) and reverse osmosis (RO) applications [1], yielding membranes with excellent properties for the removal of organic matter and salts. However, PA membrane applications are restricted due to their relatively low chemical and chlorine tolerance, and higher fouling potential [2–4]. Fouling is one of the main problems in membrane separation, which reduces efficiency, increases operational cost and shortens membrane life [5]. Therefore, it has been a long-standing goal to develop highly stable PA membranes with anti-fouling properties. Several recent investigations have considered the addition of nanomaterials as “nanofillers” in the polymer matrix to increase the anti-fouling

resistance of membranes, primarily through alterations in surface charge and hydrophobicity of membrane in surfaces water treatment applications [6–10]. Inorganic particles such as graphene oxides (GO) [11,12], carbon nanotubes (CNT) [3,13,14], silica (SiO_2) [15,16] and titanium dioxide (TiO_2) [14,17,18], when added to the PA layer of thin film composites, have been observed to improve hydrophilicity and reduce fouling. TiO_2 is one such promising nanofiller that may be used to improve properties of both the rejecting skin and support layers of membranes due to its relatively high hydrophilicity [19,20], low toxicity and environmental compatibility. While the mechanisms of improving membrane, performance are still poorly understood, TiO_2 nanoparticles appear to provide additional paths for water transport in the PA matrix [1,17]. Similarly, SiO_2 nanoparticles have received attention due to their properties of high surface energy, low cost, small particle size, large surface area, and thermal resistance. The high number of hydroxyl groups and unsaturated residual bonds on the surface of SiO_2 and the relatively inert nature of these particles make them excellent candidates for increasing membrane hydrophilicity [21–23] while being environmentally compatible [24,25]. The structure of PAs produced with TiO_2 or SiO_2 "nanofillers" typically shows a network with relatively low chain mobility, leading to a critical void size and preferred absorption on the membrane that contacts the salt water [26]. The addition of TiO_2 and SiO_2 to polymeric membranes has also been proposed as a possible strategy to reduce membrane breakage and fouling.

The current study considers the fabrication and comparison of TiO_2 and SiO_2 polymer composites porous membranes for water treatment with the goal of better understanding the properties of nanofillers, which control the membrane properties. The performance of nanocomposite membranes was evaluated using feed streams composed of salts and organic matter.

2. Material & Methods

2.1 Materials

N, N-dimethylacetamide (DMAc), isophthaloyl chloride (99 %) and benzoyl peroxide (BPO) were supplied from Sigma-Aldrich (USA). M-phenylenediamine (99 %) from Acros Organics (USA) and LiCl from Fisher (USA) were used as received. Titanium dioxide (TiO_2) nanoparticles were supplied from Nanostructured & Amorphous Materials Inc. (TX, USA), with the purity of 99.7

wt.% an average diameter of 15 nm and 240 m^2/g SSA. Silica (SiO_2) nanoparticles were supplied from Sigma Aldrich (USA) with the purity of 99.5 wt.% and an average diameter of 10-20 nm. $MgSO_4$ and NaCl were supplied from Amresco and Fisher (USA), respectively. Humic acid and Tannic acid were supplied from Alfa Aesar and Sigma Aldrich (USA), respectively.

2.2 Fabrication of membranes

Synthesis of aromatic polyamide (PA) polymer and fabrication of TiO_2 and SiO_2 composite membrane

The synthesis of membrane polymer follows an established protocol described by Hosam et. al. [26]. Briefly, a solution of m-phenylenediamine (MPD) and sodium carbonate was dissolved in deionized water. Secondly, a solution of isophthaloyl chloride (IPC) in tetrahydrofuran (THF) was rapidly poured into the MPD solution and vigorous stirring was continued for 5 min. In the mixture of MPD/IPC solution, the product thus obtained is a white fibrous precipitate. Then, the residue was separated by filtration, washed with excess deionized water and then dried under vacuum at 80–90 °C. TiO_2 and SiO_2 PA nanocomposite membranes were fabricated using the same method by introducing them into the initial MPD solution.

TiO_2 and SiO_2-PA composite membranes were fabricated using that polymer and TiO_2/SiO_2 nanoparticles having radii was about 15 nm, 10-20 nm, respectively as measured by dynamic light scattering and electron microscopy. Nanoscale TiO_2 and SiO_2 were chosen based on their differences in zero-point-of-charge (zpc) (approximately 6.5 and 2 respectively) in aqueous solutions and the ease of dispersing these nanoparticles in the solvent.

2.3 Characterization of membranes

SEM and FTIR confirmed the homogenous distributions of the nanoparticles throughout the membrane matrix. The fabricated membranes were characterized with respect to electrokinetic measurements of streaming potential, contact angle and permeability of DI water and rejection of salts and organic matter. Membrane samples were rinsed with deionized water and then dried before all analysis. Fourier transform infrared (FTIR) spectroscopy (Nicolet 8700, ThermoScientific, USA) with an Attenuated Total Reflection (ATR) unit (ZnSe crystal, 45°) was used to characterize of functional groups on the membranes at 25 °C. The hydrophilicity of the

membranes was determined by contact angle measurement (Kruss EasyDrop Goniometer, Hamburg, Germany). Membrane morphology was evaluated using Superscan SSX-550 scanning electron microscopy (SEM) (Shimadzu Co., Kyoto, Japan). Membrane streaming potential was measured by using an electrokinetic analyzer (SurPAS, Anton Paar GmbH), based on the streaming potential measurement, where 1 mM KCl was used as electrolyte solution at pH = 6 to 8.

2.4 Permeability and rejection measurements of membranes

Water permeability experiments determined the hydraulic resistance of the PA membrane, as measured of a period of 1 h over an applied range of pressures of 3.0, 3.5 and 4.0 MPa. All experiments are performed in the in Sterlitech stirred cells at 25 °C having an active membrane area of 14.6 cm^2.

In rejection experiments, solutions of salt and/or organic matter were introduced to the membrane, using 2 g/L aqueous NaCl or $MgSO_4$ as a feed solutions at 3.5 MPa and either Humic Acid (HA) or Tannic Acid (TA). Permeate flux (J), the observed salt rejection (R) and organic matter (OM) were measured at transmembrane pressure differentials, ΔP and values of R were determined as a function of J using eq. (1).

$$J = \frac{\Delta W_{feed}}{A_m \Delta t} \qquad (1)$$

Where ΔW_{feed} is the weight change of the feed solution, A_m is the membrane effective area, and Δt is the permeation time. The observed rejection, R as a function of the permeate flux, J, for all permeate sampling times is given by:

$$R = 1 - \frac{C_p}{C_f} \qquad (2)$$

Here, C_f and C_p are the salt concentration in the feed and permeate, respectively. The concentrations of salts ($MgSO_4$, NaCl) in the feed and permeate were measured using a conductivity probe (XL 20, Fisher Scientific, USA). Natural Organic Matter (NOM) rejection of the prepared membranes was evaluated by using feed solutions of either humic acid (HA) or tannic acid (TA) at a concentration of 5 mgC/L TOC content, filtered through the membranes at 3.0 MPa.

NOM substances of the feed and permeate were measured by a total organic carbon (TOC). TOC measurements performed with a Schimadzu TOC VCP-N analyzer equipped with an auto sampler.

2.5 Fouling behavior of membranes

The fouling behavior of the membranes was evaluated by filtering HA or TA solutions at room temperature for 5 h at 3.0 MPa. A concentration of 5 mg/L as organic carbon was used in both cases, selected to ensure significant fouling and corresponding to a high-NOM containing lake water. Before introducing the NOM in the feed, the initial permeability of the membrane was determined by DI water flux over a period of 30 minutes at 3.0 MPa. The initial water flux (J_1), was then compared with the flux obtained after filtering the NOM solutions (J_2) and again subsequent to NOM solution, when DI water was re-introduced to the feed for a 30 minute period at 3 MPa (J_3). In order to evaluate the fouling and fouling reversal properties of the membranes, the flux recovery ratio (FRR) and flux decline ratio (FDR) were calculated as

$$\mathrm{FRR}(\%) = \frac{J_3}{J_1} \times 100\% \qquad (3)$$

$$\mathrm{FDR}(\%) = \left(1 - \frac{J_2}{J_1}\right) \times 100\% \qquad (4)$$

3. Results & Discussion

3.1 Influence of nanoparticles on membrane properties

Surface Chemical Structure

Functional groups on PA and the molecular structure of all membranes were characterized using FTIR Spectroscopy as shown in Fig. 1. These spectra demonstrate the presence of typical PA chemical functional groups in the range of $675\ \mathrm{cm}^{-1}$- $4000\ \mathrm{cm}^{-1}$ [27]. The peaks between $1500\ \mathrm{cm}^{-1}$ and $1700\ \mathrm{cm}^{-1}$ are attributed to the PA layer [28]. Precisely, the peak at $1652\ \mathrm{cm}^{-1}$ shows succesfully formation of interfacial polymerization (IP) and the presence $\mathrm{C}=\mathrm{O}$ stretching vibration (amide I bands), band of polyamide group. The peak at 1610 and $1487\ \mathrm{cm}^{-1}$ belongs

to aromatic amide ring breathing and the peak at 1539 cm^{-1} is associated (mainly) with $N-H$ bending as well as the $C-N$ stretching vibration (amide II bands) of the $-CO-NH-$ group and at 1249 cm^{-1} (amide III bands) [27–36]. Also, the peak at 3317 cm^{-1} can be assigned to $N-H$ (and $O-H$). Fig. 1 also shows that the FTIR spectra for membranes with different ratios of TiO_2 and SiO_2 are almost identical with that of the control membrane. TiO_2 added to the layer does not appear to form any new chemical bonds as there was no difference of the wave number. However, one possible interaction between TiO_2 and carboxylic groups on the PA is suggested by formation of H-bond [37]. Overall, the IR spectra revealed that the PA layer was formed even though there was a significant change with TiO_2 addition. The characteristic vibrational bands of $Si-O-Si$ hydrolyzed from silica were also observed at 1095 cm^{-1}. As the ratio of SiO_2 nanoparticles incremented, the depth of $Si-O-Si$ peak gradually increased intensity in the FTIR spectra of the SiO_2 membranes, which confirming the successful addition of SiO_2 [38] (data not shown). As reported previously, hydrogen-bonding between hydroxyl group present at the TiO_2 and SiO_2 nanoparticles and the polyamide polymer is expected [20].

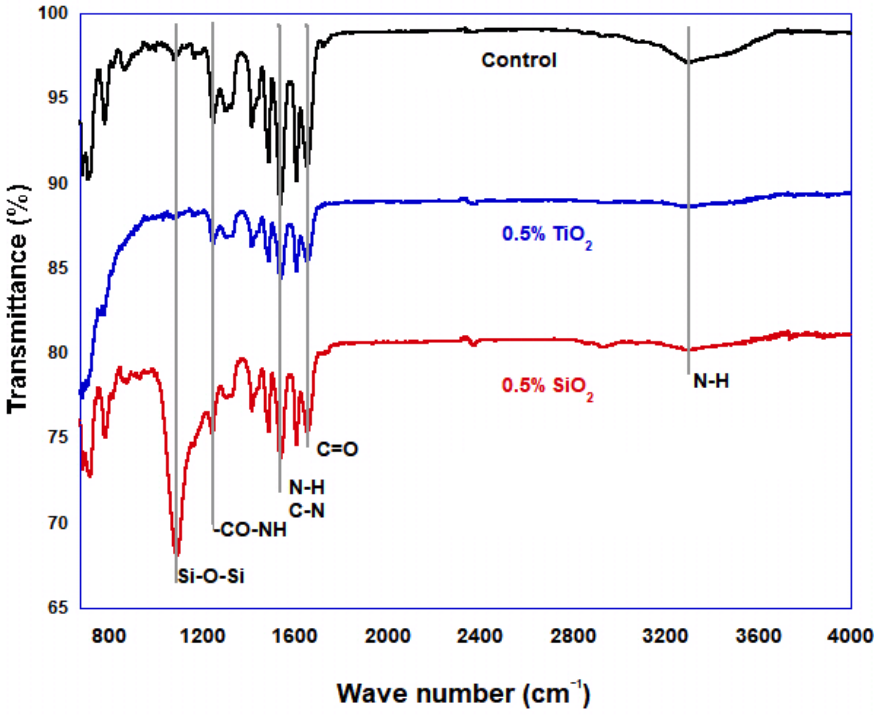

Figure 1. FTIR spectra of Control and TiO_2/SiO_2 added membranes.

Streaming potential of composite membrane

Membrane surface charge was analyzed over a pH range of 6.0 - 8.0 representative of natural surface water pH [39–42] using streaming current measurements. As seen in Figure 2, all the membranes investigated were negatively charged. Nanoparticle addition modified the membrane streaming potentials, confirming the nanoparticles addition and their presence at the membrane surface. The point of zero charge (PZC) for SiO_2 and TiO_2 is close to pH 2 [43] and pH 6.5 [44], respectively. As a consequence, at the pH values between 6 to 8 used in these experiments, the SiO_2 surface presents a more negative surface charge than does the TiO_2 with an overall effect on membrane charge. As a consequence, the SiO_2 added membranes presented the most negatively charged surface as the SiO_2 content increased. In comparison to the control membrane, the TiO_2 membrane show a more negative surface from pH 6 to 7 but a similar charge from pH 7.5 to 8, which could signify that the PZC pH of this specific TiO_2 could be close to pH 7.5.

SiO_2 nanofiller resulted in membranes that were most negatively charged with progressively more negatively charged hydroxyl groups [16] as the SiO_2 content increased. The addition of nanoparticles changed the membrane surface chemistry, at pH values > 7; TiO_2 membrane composites had similar streaming potentials to the control membrane. However, at pH values < 7; TiO_2 addition resulted in membranes that were more negatively charged than the control membranes.

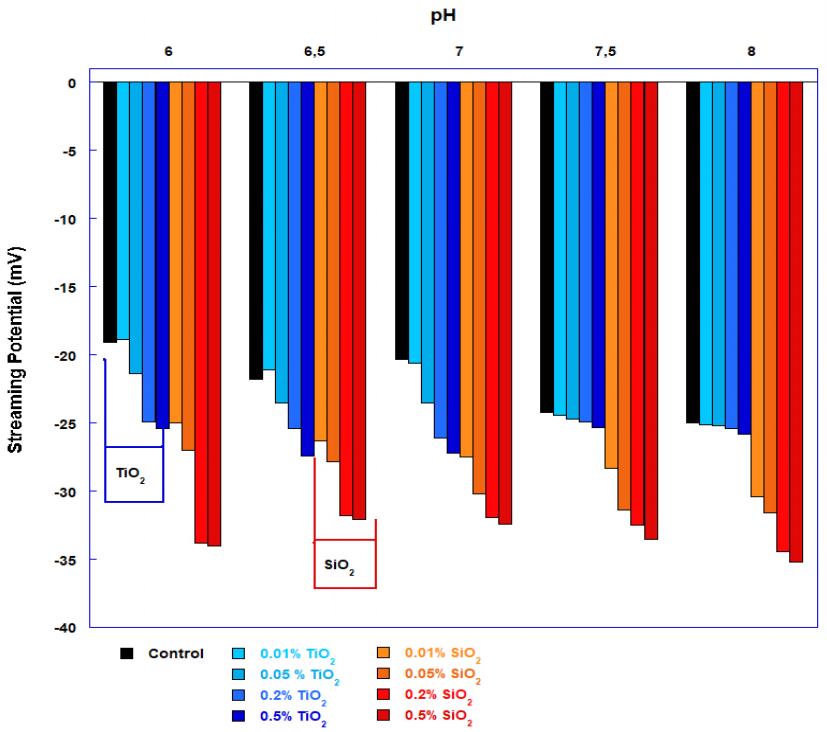

Figure 2. Streaming potential of Control and TiO_2/SiO_2 added membranes from pH 6 to 8.

Surface Hydrophilicity

Increased surface charge should be accompanied by increased hydrophilicity. Hydrophilicity of the composite membranes was evaluated by contact angle measurements between the membrane surface and the air–water crossing point [45] in Fig. 3. The control membrane showed the highest contact angle of 58°, implicating that it is the least hydrophilic of all of the membranes tested. Compared with the control, contact angles of the TiO_2 and SiO_2 membranes decreased to 38.7° and 28° for 0.5 TiO_2 and 0.5 SiO_2, respectively. Consistent with expectations, nanoparticles addition therefore creates more hydrophilic surfaces of the composite membranes due to the hydrophilic $-OH$ groups of TiO_2 and SiO_2. These results imply the presence of nanoparticles at the water interface, and not only embedded in the PA matrix. It can be found that the contact angle of both TiO_2 - and SiO_2 - doped membranes diminished with an increase in the np/PA ratio. At the same ratio, the SiO_2 membranes created a more-hydrophilic surface than TiO_2 and stronger hydrophilicity may be associated with a higher membrane permeability, assuming an identical porous network [15].

Membrane water permeability increased as the water contact angle rises. Water permeability rose by 130 % and 320 % for 0.5 TiO_2 and 0.5 SiO_2 respectively compared to the control membrane. It should be noted that a poor linear relationship was found between the contact angle and the water permeability. The 0.2 TiO_2 membrane and 0.01 SiO_2 membrane have the same contact angle and a similar water permeability. However, 0.5 TiO_2 and 0.05 SiO_2 yielded a similar contact angle but 0.05 SiO_2 water permeability was 157 % higher. This may reflect three dimensionally modification of the membrane porous network when adding high concentration of SiO_2.

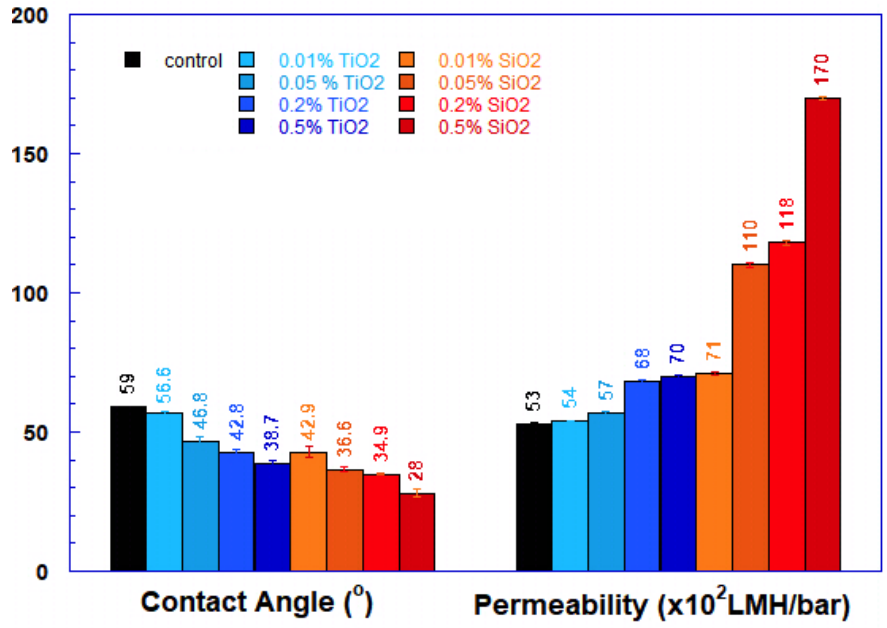

Figure 3. Contact Angle and Permeability measurements of Control and TiO_2/SiO_2 added Nanocomposite membranes.

Membrane Morphologies

Representative SEM cross-sectional images of PA membranes are presented in Fig. 4. All of the fabricated membranes showed an asymmetric porous structure, a skin layer as the selective barrier, a finger-like substructure, and a sponge-like bottom support. Also, this shows that TiO_2 and SiO_2 are well-dispersed and, due to a homogeneous casting solution, have a similar structure to the Control membrane. However, nanoparticles addition was shown to modify the membrane structure. To better understand the pore structure of the cross section of the fabricated membranes, enlarged images of skin layer cross sections were captured at 20,000x and 200,000x magnification. Additional images are presented in the SI. As can be seen in 200,000x magnification, the Control

membrane exhibited a denser structure of its skin layer. When increasing the TiO_2 and SiO_2 concentration the porous network was enlarged (Figure SII). No difference was observed between the TiO_2 and SiO_2 membranes. This difference in membrane structure may be explained by the effects of hydrophilic TiO_2 and SiO_2 nanoparticles on the rate of exchange between solvent and water during phase inversion. During, phase inversion, the casting solution is rapidly solidified at the interface between solvent and water due to the concentration gradient of the components. Notably, the literature shows that the addition of hydrophilic CNCs and CNTs may increase the rate of demixing by increasing the thermodynamic instability, leading to the membranes with higher porosity, pore radius, and surface porosity [46]. Higher hydrophilicity additives would be expected to result in a larger porous network. This observation is in accordance with the hypothesis that SiO_2 addition leads to the increased pore network modification developed in the previous section (Fig.4 (F and I)). TiO_2 and SiO_2 addition significantly modify the polyamide hydrophilicity and pore structure resulting in an increase of the water permeability [20,47,48].

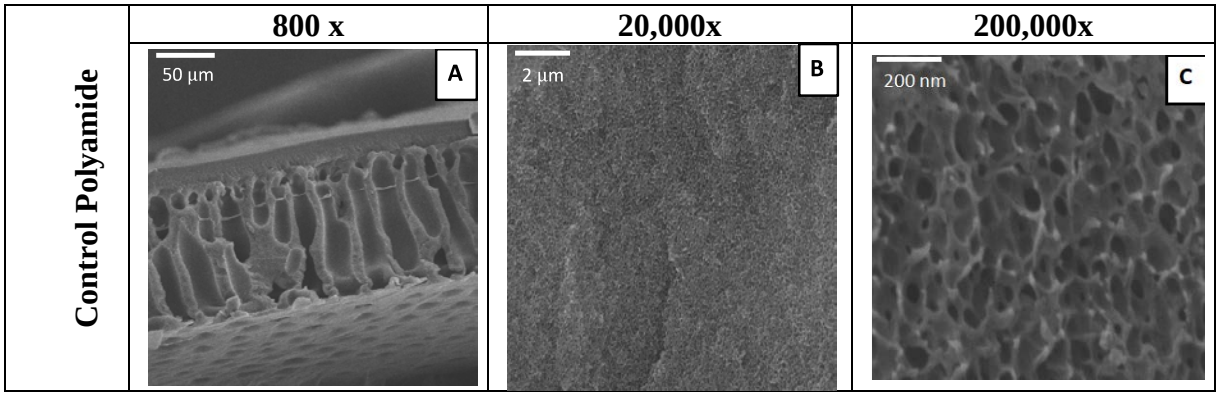

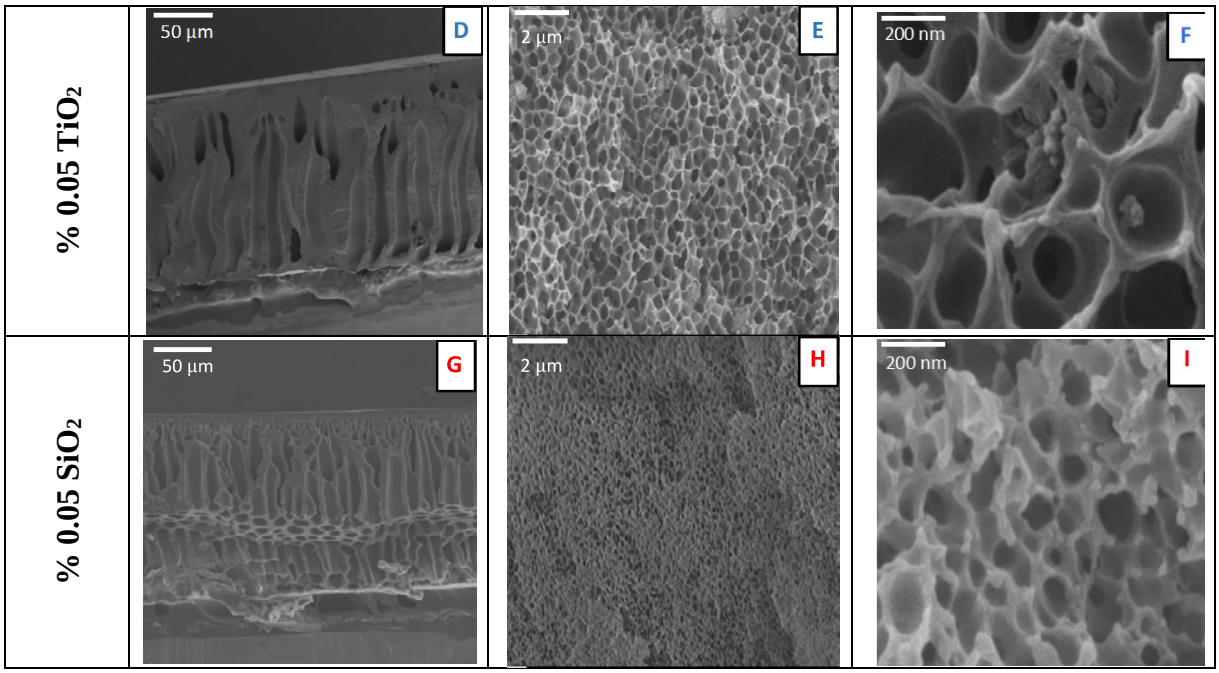

Figure 4. Cross-sectional SEM images of the all fabricated polyamide membranes.

3.2 Salt and NOM Separation and Fouling Behavior

Salt and NOM separation and flux performance of membranes

The effect of TiO_2 and SiO_2 addition on the $MgSO_4$ and NaCl rejection and permeate flux of the composite membranes is shown in Fig.5. Water flux of $MgSO_4$ and NaCl follow the same trend as the pure water flux describe earlier. The water flux follows this trend $J_{control} < J_{TiO_2} < J_{SiO_2}$ with a rise of flux when the nanoparticle content rises. The membrane flux of the $MgSO_4$ solution increased from 16.5 LMH to 20.1 LMH for % 0.01 TiO_2 and % 0.5 TiO_2, respectively and from 21.2 LMH to 41.4 LMH for % 0.01 SiO_2 and % 0.5 SiO_2, respectively.

$MgSO_4$ rejection for both nanocomposite membranes was always higher than that of the control membrane (Fig.5 B). Interestingly, increases in rejection of $MgSO_4$ for both nanofillers were relatively insensitive to changes in nanofiller content. $MgSO_4$ rejection increased by 80% and 20% for 0.01 TiO_2 and 0.01 SiO_2 respectively, to reach values of 47.7% and 31.9%, when averaged over the nanofiller amounts. In contrast, NaCl rejection was lower than that for divalent ions, with a membrane rejection between 22.4% and 31.2%, the presence of SiO_2 nanofiller appearing to reduce rejection of this monovalent salt. Between membranes, even less variability was observed

in comparison to the $MgSO_4$ rejection performance (Fig. 5. B). TiO_2 addition slightly improved the membrane performance; however, no trend can be seen with the nanoparticle's content. More SiO_2 added yielded a less NaCl rejection with the 0.5% SiO_2 reducing rejection by 14 % in comparison to the control membrane. Li et. al. reported similar results in their study with a mesoporous SiO_2 used as nanofiller in TFN PA membranes. They reported an increase in flux of 30%, with a decrease in rejection of 13% in $MgSO_4$ [49]. Also, Hu et al. added silica and found with 0.2% silica a 42.7 % higher water flux compared the control and reported promising capability for softening concentrated seawater from 8 to 20% [50]. Raejaen et al. in their study with 0.005% TiO_2 addition, observed NaCl rejection increased to 54% and flux also enhanced [19]. They also reported that with increasing concentration of TiO_2 from 0.005 to 0.1 wt.% there was a change in the pore size and thickness/porosity ratio, which caused lower permeability and stable rejection in the solute.

Hydrated ion size exclusion and Donnan effects have been suggested as mechanisms for salts rejection in similar PA membranes [51]. Because of the charge and size (Table 1) of divalent ions, divalent ions should be removed by the membrane to a greater extent by these two mechanisms than monovalent ions. The higher negative surface charge of SiO_2 membrane compared with the TiO_2 membrane at the pH values used in these experiments would be expected to create a greater Donnan effect and greater $MgSO_4$ rejection, where the opposite trend (SiO_2> TiO_2> control) was observed here. It is not clear therefore that difference in membrane charge produced by nanofillers can explain the difference in divalent ion rejection as a Donnan effect. Also, rejection increases despite the looser porous network produced by nanofillers which brings into question the role of ion, or hydrated ion exclusion.

Table 1. Physical properties of the salt ions.

Ion	Stokes Radius (nm)	Hydrated Radius (nm)
Cl^-	0.121	0.332
Na^+	0.184	0.358
SO_4^{-2}	0.230	0.379
Mg^{+2}	0.347	0.428

Indeed, the lower rejection of NaCl by the membranes with SiO_2 nanofiller is consistent with the higher permeate flux of these membranes.

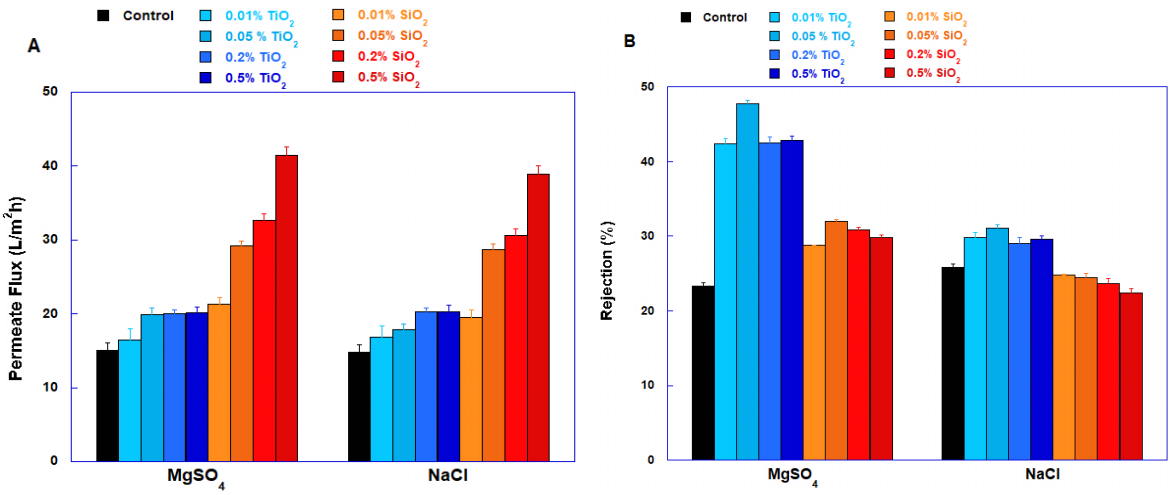

Figure 5. Comparison of all membranes with regard to $MgSO_4$ and NaCl (a) Permeate flux and (b) Rejection obtained at 35 bar.

The rejection and average flux of NOM would be expected to be more dependent on pore size than the NOM molecular weight. While the addition of nanofiller tended to increase the permeate flux when treating solutions of both HA and TA, nanofiller addition had almost no effect on NOM removal and may have even decreased the removal of the smaller molecular weight TA (Fig. 6).

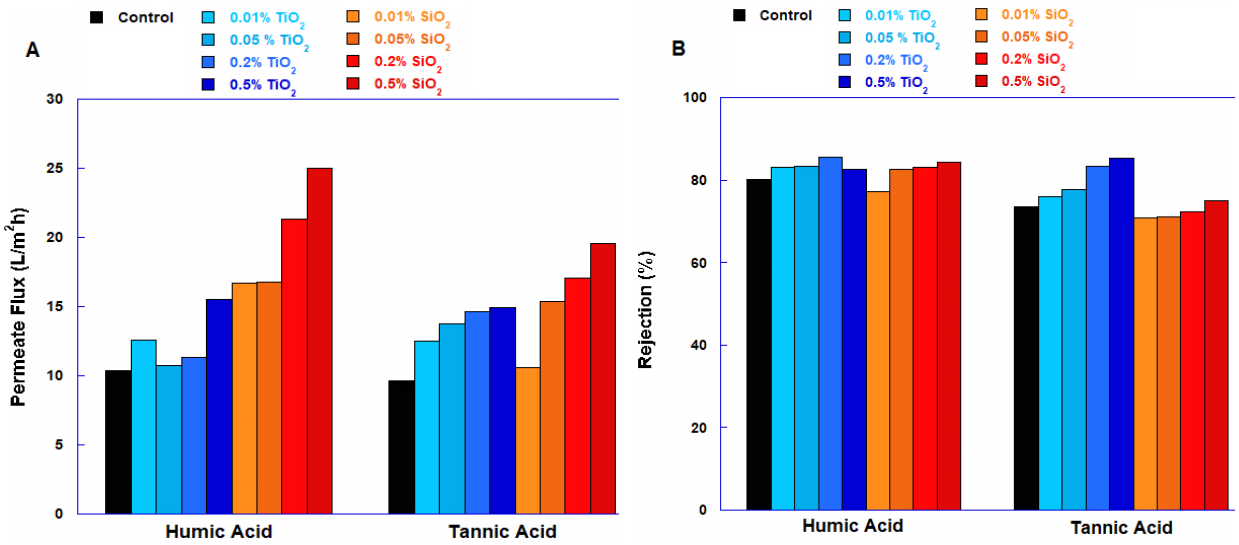

Figure 6. Humic and Tannic acid (a) Permeate flux and (b) Rejection results as a function of the nanoparticle concentration and type for membranes.

Fouling behavior

Even after normalizing for the higher initial fluxes of the membranes with nanofillers, these membranes exhibited reduced fouling during NOM filtration and improved permeate flux recovery when DI water was re-introduced (Fig. 7). Also, increases in nanofiller tended to be associated with improvements in performance (less fouling, better permeate flux recovery, Figure 8). However, the improvements were more evident in experiments with the HA. The humic acid used in this study was soil based and has a higher molecular weight and hydrophobicity than aquatic OM [52]. The TA is more hydrophilic and characterized by a smaller molecular weight (1700 Da) [53]. Both OM sources are negatively charged owing to dominance of carboxylic acid groups [54]. Changes in fouling behavior associated with changes in membrane charge would therefore be expected to be more evident with the TA. However, the TA, when introduced to the more permeable SiO_2 nanocomposite membranes, yielded the smallest improvements in reduced fouling compared with the control. It is reasonable to conclude that the increased hydrophilicity (and charge) of the membranes with nanofiller reduced fouling, but that increases in membrane permeability (and therefore pore size) increased the accessibility of the smaller molecular weight TA to the membrane interior. There may be an optimum in nanofiller content that reflects the balance between hydrophilicity/charge and membrane pore size.

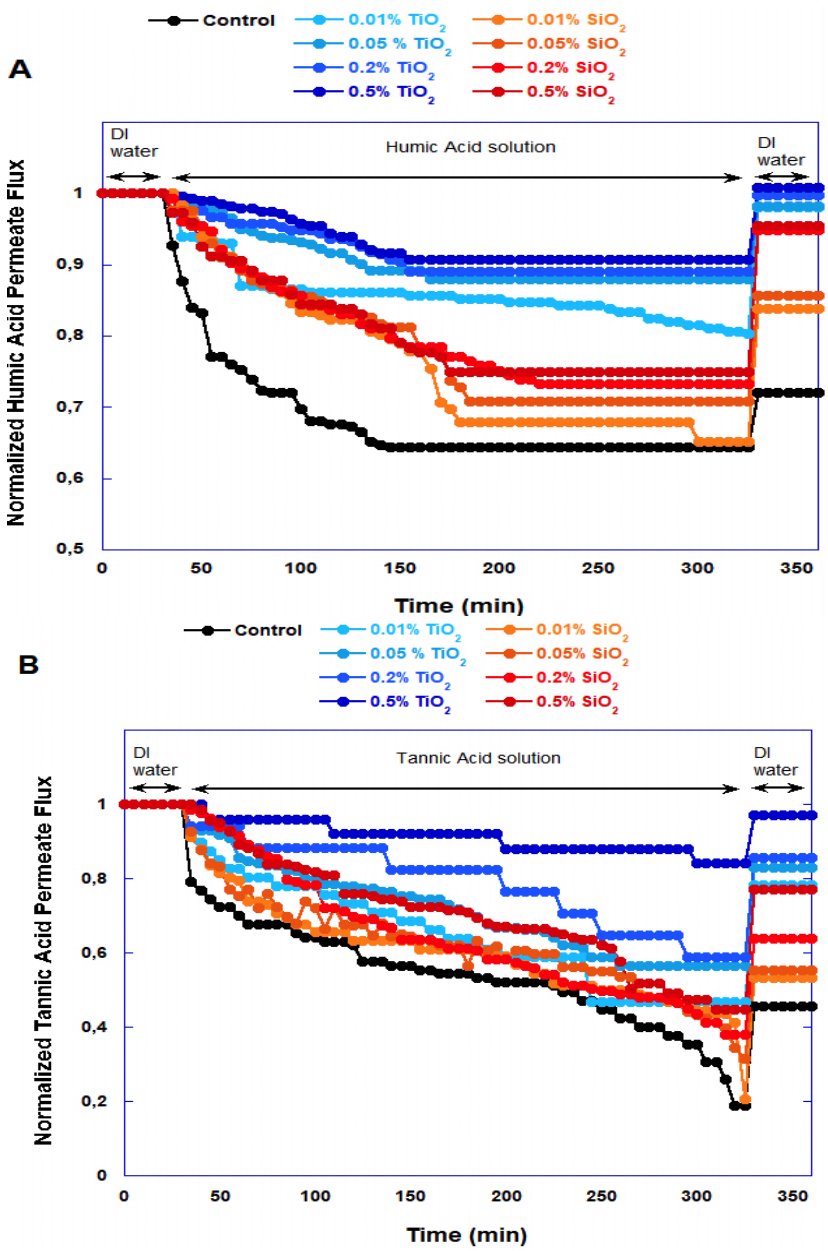

Figure 7. Normalized permeate flux as a function of permeate collected at the end of 360 minutes Humic acid (A) and Tannic acid (B) filtration for the Control and TiO_2/SiO_2 added membranes.

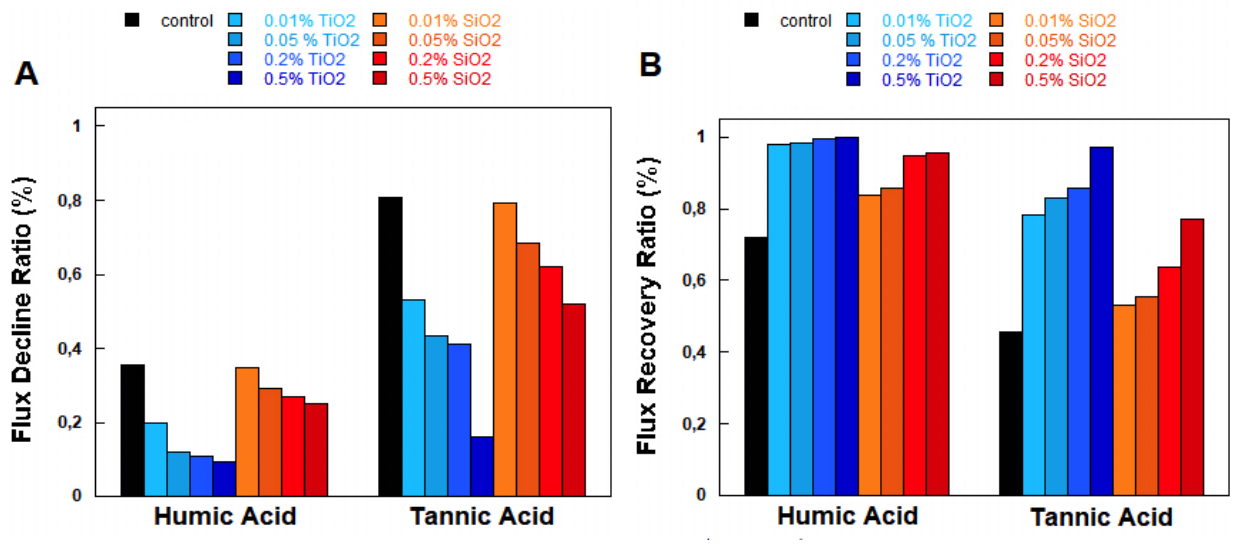

Figure 8. (A)Flux Decline Ratio (FDR) and (B)Flux Recovery Ratio (FRR) values of all membranes.

These results are consistent with many previous studies [55–57] reporting that the antifouling properties of membranes improves with decreased membrane pore size [58], increased surface hydrophilicity (and charge [55]) and a decrease of membrane roughness [57].

4. Conclusion

The comparison of the performance and morphology was carried out between control and nanocomposite membranes with nanosized particles of similar size. The addition of TiO_2 and SiO_2 to the PA membranes improved permeability and increased $MgSO_4$ rejection. Membrane permeate fluxes were increased with increasing TiO_2 and SiO_2 content up to 0.5 wt.%. The following rejection trend was observed among all of the investigated membranes: $R_{HA}>R_{TA}>R_{MgSO_4}>R_{NaCl}$. $MgSO_4$ rejection increased with the increment of TiO_2 and SiO_2 content in the membrane. NaCl rejection was similar at lower contents of TiO_2 and SiO_2. However, membranes with higher amounts of the SiO_2 content decreased NaCl rejection. HA and TA flux recovery ratio increased with the addition of TiO_2 and SiO_2 in the membrane.

The addition of metal oxide nanofillers to polyamide membranes can improve membrane performance as measured by the rejection of solutes, permeate flux, and reduced fouling. Nanoparticle charge appears to play a key role in modifying the polyamide matrix to become more hydrophilic while increasing pore size. Nanoparticles with a lower pH zpc appear to create more

highly charged and hydrophilic membranes than NPs with a higher pH zpc. Lower pH zpc also appears to favor a larger pore size in the composite membrane. Many of these effects are dependent on the concentration of nanofiller, suggesting that there is an optimal nanofiller content to be considered in formulating membranes to achieve a balance between hydrophilicity and pore size that may vary as a function of the feedwater quality.

Acknowledgement

GMUB would like to thank for funding provided by TUBITAK-BIDEB 2214-A International Research Fellowship Programme. This work was also partially funded through the Center for the Environmental Implications of NanoTechnology (CEINT) under NSF Cooperative Agreement Number EF-0830093, and the NSF Partnership in International Research and Education (PIRE) program.

References

[1] W.J. Lau, S. Gray, T. Matsuura, D. Emadzadeh, J. Paul Chen, A.F. Ismail, A review on polyamide thin film nanocomposite (TFN) membranes: History, applications, challenges and approaches, Water Res. 80 (2015) 306–324. doi:10.1016/j.watres.2015.04.037.

[2] X. Li, Y. Chen, X. Hu, Y. Zhang, L. Hu, Desalination of dye solution utilizing PVA/PVDF hollow fiber composite membrane modified with TiO2nanoparticles, J. Memb. Sci. 471 (2014) 118–129. doi:10.1016/j.memsci.2014.08.018.

[3] H.J. Kim, K. Choi, Y. Baek, D.G. Kim, J. Shim, J. Yoon, J.C. Lee, High-performance reverse osmosis CNT/polyamide nanocomposite membrane by controlled interfacial interactions, ACS Appl. Mater. Interfaces. 6 (2014) 2819–2829. doi:10.1021/am405398f.

[4] H. Wu, X.L. Chen, X. Huang, H.M. Ruan, Y.L. Ji, L.F. Liu, C.J. Gao, A novel semi-aromatic polyamide TFC reverse osmosis membrane fabricated from a dendritic molecule of trimesoylamidoamine through a two-step amine-immersion mode, RSC Adv. 7 (2017) 39127–39137. doi:10.1039/c7ra07298h.

[5] B. Van der Bruggen, M. M??ntt??ri, M. Nystr??m, Drawbacks of applying nanofiltration and how to avoid them: A review, Sep. Purif. Technol. 63 (2008) 251–263. doi:10.1016/j.seppur.2008.05.010.

[6] N. Hilal, H. Al-Zoubi, N.A. Darwish, A.W. Mohammad, M. Abu Arabi, A comprehensive review of nanofiltration membranes: Treatment, pretreatment, modelling, and atomic force microscopy, Desalination. 170 (2004) 281–308. doi:10.1016/j.desal.2004.01.007.

[7] F.N.S. Yavuz, R. Sengur Tasdemir, T. Turken, G.M. Urper, I. Koyuncu, Improvement of anti-biofouling properties of hollow fiber membranes with bismuth-BAL chelates (BisBAL), Environ. Technol. (United Kingdom). (2017). doi:10.1080/09593330.2017.1377292.

[8] A. Anand, B. Unnikrishnan, J.Y. Mao, H.J. Lin, C.C. Huang, Graphene-based nanofiltration membranes for improving salt rejection, water flux and antifouling–A review, Desalination. 429 (2018) 119–133. doi:10.1016/j.desal.2017.12.012.

[9] C.Y. Tang, T.H. Chong, A.G. Fane, Colloidal interactions and fouling of NF and RO membranes: A review, Adv. Colloid Interface Sci. 164 (2011) 126–143. doi:10.1016/j.cis.2010.10.007.

[10] R. Epsztein, E. Shaulsky, N. Dizge, D.M. Warsinger, M. Elimelech, Role of Ionic Charge Density in Donnan Exclusion of Monovalent Anions by Nanofiltration, Environ. Sci. Technol. 52 (2018) 4108–4116. doi:10.1021/acs.est.7b06400.

[11] H. Zhang, Bin Li, J. Pan, Y. Qi, J. Shen, C. Gao, B. Van der Bruggen, Carboxyl-functionalized graphene oxide polyamide nanofiltration membrane for desalination of dye solutions containing monovalent salt, J. Memb. Sci. 539 (2017) 128–137. doi:10.1016/j.memsci.2017.05.075.

[12] S. Bano, A. Mahmood, S.-J. Kim, K.-H. Lee, Graphene oxide modified polyamide nanofiltration membrane with improved flux and antifouling properties, J. Mater. Chem. A. 3 (2015) 2065–2071. doi:10.1039/C4TA03607G.

[13] E.A. Genceli, R. Sengur-Tasdemir, G.M. Urper, S. Gumrukcu, Z. Guler-Gokce, U. Dagli, T. Turken, A.S. Sarac, I. Koyuncu, Effects of carboxylated multi-walled carbon nanotubes having different outer diameters on hollow fiber ultrafiltration membrane fabrication and characterization by electrochemical impedance spectroscopy, Polym. Bull. 75 (2018) 2431–2457. doi:10.1007/s00289-017-2155-3.

[14] G.M. Urper-Bayram, B. Sayinli, N. Bossa, E. Ngaboyamahina, R. Sengur-Tasdemir, E. Ates-Genceli, M. Wiesner, I. Koyuncu, Thin film nanocomposite nanofiltration hollow fiber membrane fabrication and characterization by electrochemical impedance spectroscopy, Polym. Bull. (2019). doi:10.1007/s00289-019-02905-w.

[15] N. Niksefat, M. Jahanshahi, A. Rahimpour, The effect of SiO2nanoparticles on morphology and performance of thin film composite membranes for forward osmosis application, Desalination. 343 (2014) 140–146. doi:10.1016/j.desal.2014.03.031.

[16] L.M. Jin, S.L. Yu, W.X. Shi, X.S. Yi, N. Sun, Y.L. Ge, C. Ma, Synthesis of a novel composite nanofiltration membrane incorporated SiO2nanoparticles for oily wastewater desalination, Polymer (Guildf). 53 (2012) 5295–5303. doi:10.1016/j.polymer.2012.09.014.

[17] A. Sotto, A. Boromand, S. Balta, S. Darvishmanash, J. Kim, B. Van der Bruggen, Nanofiltration membranes enhanced with TiO_2 nanoparticles: a comprehensive study, Desalin. Water Treat. 34 (2011) 179–183. doi:10.5004/dwt.2011.2787.

[18] G.M. Urper-Bayram, B. Sayinli, R. Sengur-Tasdemir, T. Turken, E. Pekgenc, O. Gunes, E. Ates-Genceli, V. V. Tarabara, I. Koyuncu, Nanocomposite hollow fiber nanofiltration

membranes: Fabrication, characterization, and pilot-scale evaluation for surface water treatment, J. Appl. Polym. Sci. 136 (2019) 1–8. doi:10.1002/app.48205.

[19] B. Rajaeian, A. Rahimpour, M.O. Tade, S. Liu, Fabrication and characterization of polyamide thin film nanocomposite (TFN) nanofiltration membrane impregnated with TiO2nanoparticles, Desalination. 313 (2013) 176–188. doi:10.1016/j.desal.2012.12.012.

[20] S.H. Kim, S.Y. Kwak, B.H. Sohn, T.H. Park, Design of TiO2nanoparticle self-assembled aromatic polyamide thin-film-composite (TFC) membrane as an approach to solve biofouling problem, J. Memb. Sci. 211 (2003) 157–165. doi:10.1016/S0376-7388(02)00418-0.

[21] C. Liu, J. Lee, C. Small, J. Ma, M. Elimelech, Comparison of organic fouling resistance of thin-film composite membranes modified by hydrophilic silica nanoparticles and zwitterionic polymer brushes, J. Memb. Sci. 544 (2017) 135–142. doi:10.1016/j.memsci.2017.09.017.

[22] G.L. Jadav, P.S. Singh, Synthesis of novel silica-polyamide nanocomposite membrane with enhanced properties, J. Memb. Sci. 328 (2009) 257–267. doi:10.1016/j.memsci.2008.12.014.

[23] T. Ormanci-Acar, F. Celebi, B. Keskin, O. Mutlu-Salmanlı, M. Agtas, T. Turken, A. Tufani, D.Y. Imer, G.O. Ince, T.U. Demir, Y.Z. Menceloglu, S. Unal, I. Koyuncu, Fabrication and characterization of temperature and pH resistant thin film nanocomposite membranes embedded with halloysite nanotubes for dye rejection, Desalination. 429 (2018) 20–32. doi:10.1016/j.desal.2017.12.005.

[24] N. Rakhshan, M. Pakizeh, The effect of functionalized SiO2nanoparticles on the morphology and triazines separation properties of cellulose acetate membranes, J. Ind. Eng. Chem. 34 (2016) 51–60. doi:10.1016/j.jiec.2015.10.031.

[25] R.G. Suthar, B. Gao, Nanotechnology for drinking water purification, Elsevier Inc., 2017. doi:10.1016/B978-0-12-804300-4.00003-4.

[26] H.A. Shawky, S.R. Chae, S. Lin, M.R. Wiesner, Synthesis and characterization of a carbon nanotube/polymer nanocomposite membrane for water treatment, Desalination. 272 (2011) 46–50. doi:10.1016/j.desal.2010.12.051.

[27] C.Y. Tang, Y.N. Kwon, J.O. Leckie, Effect of membrane chemistry and coating layer on physiochemical properties of thin film composite polyamide RO and NF membranes. I.

FTIR and XPS characterization of polyamide and coating layer chemistry, Desalination. 242 (2009) 149–167. doi:10.1016/j.desal.2008.04.003.

[28] B. Khorshidi, I. Biswas, T. Ghosh, T. Thundat, M. Sadrzadeh, Robust fabrication of thin film polyamide-TiO2nanocomposite membranes with enhanced thermal stability and anti-biofouling propensity, Sci. Rep. 8 (2018) 1–10. doi:10.1038/s41598-017-18724-w.

[29] P. Veerababu, B.B. Vyas, P.S. Singh, P. Ray, Limiting thickness of polyamide-polysulfone thin-film-composite nanofiltration membrane, Desalination. 346 (2014) 19–29. doi:10.1016/j.desal.2014.05.007.

[30] Y. Yang, H. Zeng, W.S. Huo, Y.H. Zhang, Direct Electrochemistry and Catalytic Function on Oxygen Reduction Reaction of Electrodes Based on Two Kinds of Magnetic Nano-particles with Immobilized Laccase Molecules, J. Inorg. Organomet. Polym. Mater. 27 (2017) 201–214. doi:10.1007/s10904-016-0464-x.

[31] A.H.M. El-Aassar, M.M.S. Abo Elfadl, M.E.A. Ali, Y.H. Kotp, H.A. Shawky, Effect of manufacture conditions on reverse osmosis desalination performance of polyamide thin film composite membrane and their spiral wound element, Desalin. Water Treat. 69 (2017) 65–71. doi:10.5004/dwt.2017.20293.

[32] M.M. Said, A.H.M. El-Aassar, Y.H. Kotp, H.A. Shawky, M.S.A.A. Mottaleb, Performance assessment of prepared polyamide thin film composite membrane for desalination of saline groundwater at Mersa Alam-Ras Banas, Red Sea Coast, Egypt, Desalin. Water Treat. 51 (2013) 4927–4937. doi:10.1080/19443994.2013.795208.

[33] Y.H. Kotp, Controlled synthesis and sorption properties of magnesium silicate nanoflower prepared by a surfactant-mediated method, Sep. Sci. Technol. 52 (2017) 657–670. doi:10.1080/01496395.2016.1264425.

[34] I.M. Ali, M.Y. Nassar, Y.H. Kotp, M. Khalil, Cylindrical-design, dehydration, and sorption properties of easily synthesized magnesium phosphosilicate nanopowder, Part. Sci. Technol. 37 (2019) 207–219. doi:10.1080/02726351.2017.1362607.

[35] E.R. soliman, Y.H. Kotp, E.R. Souaya, K.A. Guindy, R.G.M. Ibrahim, Development the sorption behavior of nanocomposite Mg/Al LDH by chelating with different monomers, Compos. Part B Eng. 175 (2019) 107131. doi:10.1016/j.compositesb.2019.107131.

[36] Y.H. Kotp, Removal of organic pollutants using polysulfone ultrafiltration membrane containing polystyrene silicomolybdate nanoparticles: Case study: Borg El Arab area, J.

Water Process Eng. 30 (2019) 0–1. doi:10.1016/j.jwpe.2018.01.008.

[37] A. hameed M.A. El-Aassar, Improvement of reverse osmosis performance of polyamide thin-film composite membranes using TiO<inf>2</inf> nanoparticles, Desalin. Water Treat. 55 (2015) 2939–2950. doi:10.1080/19443994.2014.940206.

[38] A. Peyki, A. Rahimpour, M. Jahanshahi, Preparation and characterization of thin film composite reverse osmosis membranes incorporated with hydrophilic SiO2nanoparticles, Desalination. 368 (2015) 152–158. doi:10.1016/j.desal.2014.05.025.

[39] L.F. Greenlee, D.F. Lawler, B.D. Freeman, B. Marrot, P. Moulin, Reverse osmosis desalination: Water sources, technology, and today's challenges, Water Res. 43 (2009) 2317–2348. doi:10.1016/j.watres.2009.03.010.

[40] G.M. Geise, D.R. Paul, B.D. Freeman, Fundamental water and salt transport properties of polymeric materials, Prog. Polym. Sci. 39 (2014) 1–24. doi:10.1016/j.progpolymsci.2013.07.001.

[41] V. V. Tarabara, I. Koyuncu, M.R. Wiesner, Effect of hydrodynamics and solution ionic strength on permeate flux in cross-flow filtration: Direct experimental observation of filter cake cross-sections, J. Memb. Sci. 241 (2004) 65–78. doi:10.1016/j.memsci.2004.04.030.

[42] M. Oćwieja, Z. Adamczyk, M. Morga, Adsorption of tannic acid on polyelectrolyte monolayers determined in situ by streaming potential measurements, J. Colloid Interface Sci. 438 (2015) 249–258. doi:10.1016/j.jcis.2014.09.071.

[43] X. Song, N. Jiang, Y. Li, D. Xu, G. Qiu, Synthesis of CeO2-coated SiO2 nanoparticle and dispersion stability of its suspension, Mater. Chem. Phys. 110 (2008) 128–135.

[44] J.F. Budarz, E.M. Cooper, C. Gardner, E. Hodzic, P.L. Ferguson, C.K. Gunsch, M.R. Wiesner, Chlorpyrifos degradation via photoreactive TiO2 nanoparticles: assessing the impact of a multi-component degradation scenario, J. Hazard. Mater. 372 (2019) 61–68.

[45] C.F. de Lannoy, D. Jassby, D.D. Davis, M.R. Wiesner, A highly electrically conductive polymer-multiwalled carbon nanotube nanocomposite membrane, J. Memb. Sci. 415–416 (2012) 718–724. doi:10.1016/j.memsci.2012.05.061.

[46] L. Bai, N. Bossa, F. Qu, J. Winglee, G. Li, K. Sun, H. Liang, M.R. Wiesner, Comparison of Hydrophilicity and Mechanical Properties of Nanocomposite Membranes with Cellulose Nanocrystals and Carbon Nanotubes, Environ. Sci. Technol. 51 (2017) 253–262. doi:10.1021/acs.est.6b04280.

[47] M.L. Lind, D. Eumine Suk, T.-V. Nguyen, E.M. V Hoek, Tailoring the structure of thin film nanocomposite membranes to achieve seawater RO membrane performance, Environ. Sci. Technol. 44 (2010) 8230–8235.

[48] M.L. Lind, A.K. Ghosh, A. Jawor, X. Huang, W. Hou, Y. Yang, E.M. V Hoek, Influence of zeolite crystal size on zeolite-polyamide thin film nanocomposite membranes, Langmuir. 25 (2009) 10139–10145.

[49] Q. Li, Z. Li, H. Yu, X. Pan, X. Wang, Y. Wang, J. Song, Effects of ordered mesoporous silica on the performances of composite nanofiltration membrane, Desalination. 327 (2013) 24–31. doi:10.1016/j.desal.2013.08.002.

[50] D. Hu, Z.-L. Xu, C. Chen, Polypiperazine-amide nanofiltration membrane containing silica nanoparticles prepared by interfacial polymerization, Desalination. 301 (2012) 75–81.

[51] Y. Roy, D.M. Warsinger, J.H. Lienhard, Effect of temperature on ion transport in nanofiltration membranes: Diffusion, convection and electromigration, Desalination. 420 (2017) 241–257. doi:10.1016/j.desal.2017.07.020.

[52] W. Yuan, A.L. Zydney, Humic acid fouling during ultrafiltration, Environ. Sci. Technol. 34 (2000) 5043–5050. doi:10.1021/es0012366.

[53] M. Campinas, M.J. Rosa, Removal of microcystins by PAC/UF, Sep. Purif. Technol. 71 (2010) 114–120. doi:10.1016/j.seppur.2009.11.010.

[54] E.-E. Chang, P.-C. Chiang, W.-Y. Tang, S.-H. Chao, H.-J. Hsing, Effects of polyelectrolytes on reduction of model compounds via coagulation, Chemosphere. 58 (2005) 1141–1150.

[55] B.S. Lalia, V. Kochkodan, R. Hashaikeh, N. Hilal, A review on membrane fabrication: Structure, properties and performance relationship, Desalination. 326 (2013) 77–95. doi:10.1016/j.desal.2013.06.016.

[56] S. Kang, M. Herzberg, D.F. Rodrigues, M. Elimelech, Antibacterial effects of carbon nanotubes: size does matter!, Langmuir. 24 (2008) 6409–6413.

[57] D. Rana, T. Matsuura, Surface modifications for antifouling membranes, Chem. Rev. 110 (2010) 2448–2471.

[58] L.D. Nghiem, S. Hawkes, Effects of membrane fouling on the nanofiltration of trace organic contaminants, Desalination. 236 (2009) 273–281.